Colloidal Nanocrystals with Inorganic Halide, Pseudohalide, and Halometallate Ligands

Hao Zhang,[†] Jaeyoung Jang,[†] Wenyong Liu,[†] and Dmitri V. Talapin[†,‡,*]

[†]Department of Chemistry and James Franck Institute, University of Chicago, Chicago, Illinois 60637, United States and [‡]Center for Nanoscale Materials, Argonne National Laboratory, Argonne, Illinois 60439, United States

ABSTRACT We investigate simple halides and pseudohalides as an important class of inorganic ligands for nanocrystals (NCs) in solution phase ligand exchange. These short, robust, and easy to model ligands bind to the NC surface and provide electrostatic stabilization of NC dispersions in *N*-methylformamide. The replacement of organic ligands on NCs with compact halide and pseudohalide ligands greatly facilitates electronic communication between NCs. For example, a high electron mobility of $\mu \approx 12$ cm^2 V^{-1} s^{-1} has been observed in thin films made of I$^-$-capped CdSe NCs. We also studied charge transport properties of thin films based on the pseudohalide N_3^--capped InAs NCs, suggesting the possibility of obtaining "all III–V" NC solids. In addition, we extend the surface chemistry of halometallates (*e.g.*, $CH_3NH_3PbI_3$), which can stabilize colloidal solutions of lead chalcogenide NCs. These halide, pseudohalide, and halometallate ligands enrich the current family of inorganic ligands and can open up more opportunities for applications of NCs in the fields of electronics, optoelectronics, and thermoelectrics.

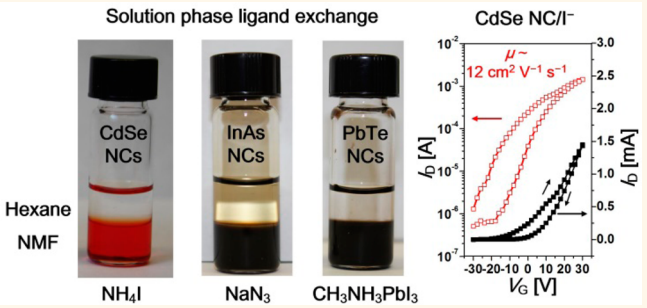

KEYWORDS: nanocrystals · surface chemistry · halide ligands · pseudohalide ligands · halometallate ligands · charge transport · carrier mobility

Colloidal nanocrystals (NCs) represent an emerging class of building blocks in various electronic,[1–3] optoelectronic,[4–7] and thermoelectric applications[8,9] due to their size- and shape-tunable optical and electronic properties as well as their solution processability. All these rely on facile injection or extraction of nonequilibrium charge carriers into or from NCs, which is related to carrier mobility (μ) in NC arrays. Therefore, as-synthesized colloidal NCs require post-treatment to remove the original long chain, insulating hydrocarbon ligands and to facilitate strong coupling between adjacent NCs.[10] Our group introduced the concept of inorganic molecular metal chalcogenide ligands (MCCs, *e.g.*, $Sn_2S_6^{4-}$, $In_2Se_4^{2-}$),[11,12] which can replace bulky organic ligands while providing colloidal stabilization and preserving quantum confinement in individual NCs. Later, simple chalcogenide ions (*e.g.*, S^{2-}, Se^{2-}, Te^{2-})[13,14] and other small charged ions (*e.g.*, SCN^-)[15] were discovered as new members of the inorganic ligand family. These advancements in ligand chemistry have spurred research on all-inorganic NC solids with record high carrier mobilities. For instance, CdSe NCs[16–19] with $\mu \approx 20$ cm^2 V^{-1} s^{-1} at 300 K, PbSe NCs[20,21] with $\mu \approx 5–10$ cm^2 V^{-1} s^{-1}, and InAs NCs[22,23] with $\mu \approx 10–15$ cm^2 V^{-1} s^{-1} have been reported, illustrating the potential use of all-inorganic NC solids in high-performance optoelectronic devices. It is interesting to note that the majority of the currently developed inorganic ligands are based on chalcogenides (or, anions binding to the NC surface through group VIA elements). Development of nonchalcogen-based inorganic ligands is important to broaden the scope of ligand functionalities (*e.g.*, redox stability) and build an extensive toolbox of surface chemistries for rational design of NC materials. This motivated us to explore new, alternative classes of cheap and robust inorganic ligands, such as halides (Cl^-, Br^-, I^-). The concept of colloidal stabilization using halide anions was reported more than a century ago when I^- was

* Address correspondence to dvtalapin@uchicago.edu.

Received for review May 6, 2014 and accepted July 2, 2014.

Published online July 02, 2014
10.1021/nn502470v

employed to stabilize AgI colloids.[24,25] A similar scenario was observed in the aqueous solution of Ag or Pd NCs with Br^- as a cosurfactant.[26] Recent studies by the Sargent group have also demonstrated the solid-state approach for replacing bulky organic ligands on lead chalcogenide (PbCh) NCs (*e.g.*, PbS) with halide anions, which offer surface passivation of NCs and contribute to high photovoltaic efficiencies.[27] On the other hand, ligand exchange in the solution phase is more attractive since it enables the formation of closely packed NC arrays with a more complete replacement of organic ligands as well as negligible volume contraction and cracking. In the solution phase, halide ligands from various sources have been employed as cosurfactants for colloidally synthesized NCs in the presence of organic ligands in nonpolar solvents (*e.g.*, Owen and Anderson *et al.*: Cl^- from Me_3SiCl[28] or $CdCl_2$[29,30] together with amines or phosphines for CdSe NCs; Sargent group: I^- from tetrabutylammonium iodide[31] together with oleic acid (OA) or Cl^- from $CdCl_2$[32,33] together with oleylamine (OAm) and tetradecylphosphonic acid for PbS NCs; Klimov group: Cl^- from Cl_2 gas[34] together with OA for PbSe or PbS NCs). During the preparation of this paper, Dirin *et al.*[35] reported the use of lead halide perovskite and other metal halide complexes in the stabilization of PbS and several other NCs (InP, Au, *etc.*), demonstrating the potential of metal halide complexes as a new class of surface ligands for NCs. The introduction of halide ligands on PbCh (Ch = S, Se) NCs has led to improved passivation of the NC surface,[27] elimination of midgap trap states,[31] n-type doping,[36] improvement in stability toward oxidation,[34] *etc*. Recently, Niu *et al*. reported the ligand exchange of CdSe and PbS NCs with methylammonium halides (CH_3NH_3X, X = Cl, Br, I) in a two-phase (heptane/methanol) system. However, the halide-capped NCs usually formed a metastable solution in formamide, especially when Cl^- or Br^- anions were employed.[37] A more attractive, one-step, facile procedure to obtain halide- or halide-related-ligand-capped NCs with good colloidal stability and solution processability has yet to be established. It is also beneficial to investigate the charge transport properties of halide-capped II–VI and III–V all-inorganic NC solids. The chemical versatility of these halide-related ligands is anticipated to provide a new avenue for optimization of electronic properties in NC-based devices.

In this work, we study simple halides (NH_4I, NH_4Br, NH_4Cl, and even NaCl or KBr) as inorganic ligands for colloidal NCs. Similar to other inorganic ligands, these halide anions bind to the electrophilic NC surface and provide electrostatic stabilization for NCs in *N*-methylformamide (NMF), which is an environmentally benign solvent with an ultrahigh dielectric constant ($\varepsilon \approx 182$). The halide ligands are rather simple, short, and abundant, while possessing enhanced stability toward air/moisture as well as reduced toxicity compared to chalcogen-based ligands. All of these features suggest a broad use of halide ligands in NC-based devices. Moreover, we extend surface chemistry to pseudohalides (*e.g.*, N_3^- or CN^-) other than the chalcogen-based SCN^- ligand developed by the Murray and Kagan group.[15,18,19] The azide ligand (N_3^-) works especially well for III–V NCs (InAs and InP). To the best of our knowledge, N_3^- is the first example of "group VA" ligands that offer an opportunity to construct "all III–V" NC solids together with III–V NCs. We harness the advantages of short halide ligands to achieve $\mu \approx 12\ cm^2\ V^{-1}\ s^{-1}$ in I^--capped CdSe NC based thin film, which is comparable to record mobilities for solution-processed NC devices. Furthermore, we explore the possibility of employing lead halide based halometallates (*e.g.*, $CH_3NH_3PbI_3$, which possesses a perovskite crystal structure) as surface ligands for PbCh NCs, especially PbTe NCs, which could be stabilized only with select MCC (Sb_2Te_3-MCC)[38] and chalcogenide (Te^{2-})[14] ligands. We believe the success of surface chemistry using halide, pseudohalide, and halometallate ligands can greatly expand the potential application areas of all-inorganic NC solids.

RESULTS AND DISCUSSION

The NCs studied in this work were synthesized following previously reported procedures using organic ligands such as octadecylphosphonic acid (ODPA), trioctylphosphine oxide (TOPO), trioctylphosphine (TOP), tributylphosphine (TBP), oleic acid (OA), and oleylamine (OAm) (see Experimental Section). To exchange the organic ligands, we combine solutions of NCs in hexane with solutions of halide, pseudohalide, or halometallate ligands in NMF. The two-phase mixture was vigorously stirred for a short period of time (from several minutes up to several hours, depending on multiple factors including the combination of organic and halide ligands as well as the concentration, size, and shape of the original NCs), after which a complete phase transfer of NCs from hexane to NMF was observed (Figure 1a). As a polar solvent with an extraordinarily high dielectric constant ($\varepsilon \approx 182$), NMF is indispensable for stabilizing NCs with short, monocharged halide or pseudohalide ligands. Other commonly used polar solvents for inorganic-capped NCs (formamide ($\varepsilon \approx 106$), dimethylformamide ($\varepsilon \approx 36$), hydrazine ($\varepsilon \approx 55$), or dimethyl sulfoxide ($\varepsilon \approx 47$)) cannot stabilize NC dispersions. In the following sections, we will summarize and discuss the results obtained from NCs capped with various halide, pseudohalide, and halometallate ligands.

Halide Ligands (I^-, Br^-, Cl^-). Figure 1c compares the absorption spectra of ~3.6 nm CdSe NCs capped with organic ligands in hexane and NH_4I in NMF. The I^--capped CdSe NCs preserved their excitonic features, indicating no changes in the size and shape of the NCs. In addition, the X-ray diffraction (XRD) pattern of the

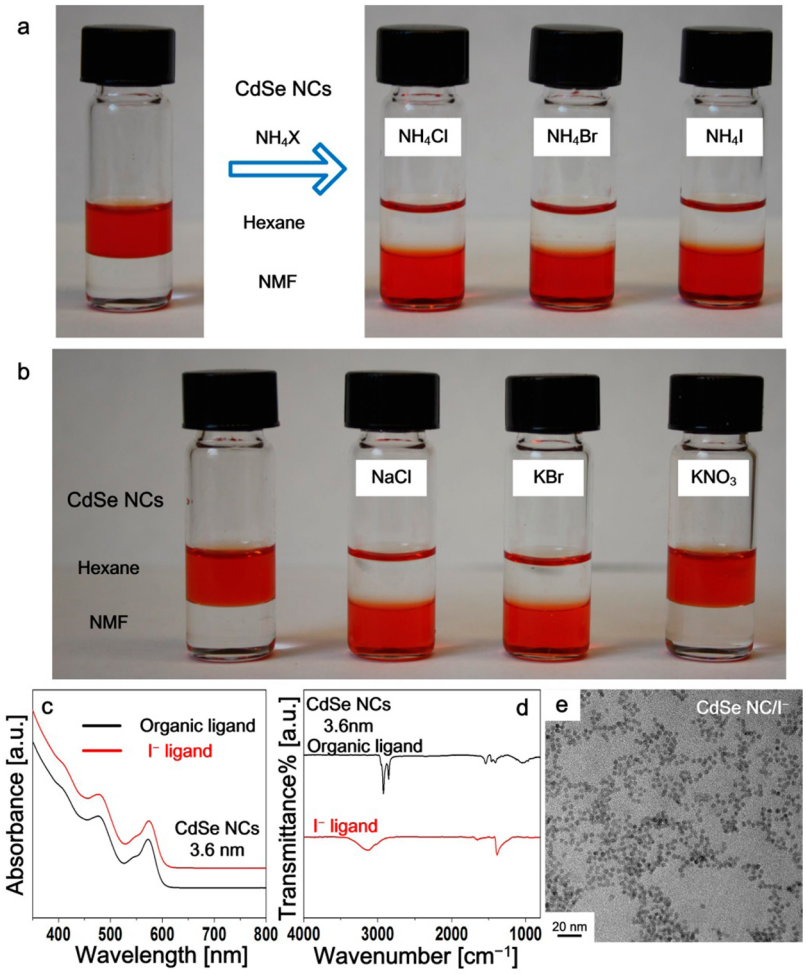

Figure 1. Red-colored colloidal solution of CdSe NCs undergoes phase transfer from hexane to NMF in the presence of (a) NH_4X (X = I, Br, Cl) and (b) NaCl or KBr. No phase transfer occurs when using KNO_3 as the ligands in NMF. (c) Absorption spectra of 3.6 nm CdSe NCs capped with organic and I^- ligands in hexane and NMF, respectively. (d) FTIR spectra of CdSe NCs capped with organic ligands and I^- from NH_4I. (e) TEM image of CdSe NCs capped with I^- ligands.

I^--capped CdSe NCs was identical to that of organically capped NCs with no reflections from I-containing phases or other impurities (Figure S1a). Fourier-transform infrared (FTIR) spectra of a dried, I^--capped CdSe NC film deposited on KBr substrates were used to monitor the completeness of ligand exchange (Figure 1d). The bands at 2800−3000 cm^{-1} corresponding to the C−H stretching almost completely disappeared after ligand exchange. Instead, I^--capped CdSe NCs showed broad bands at ∼3400 and 1400 cm^{-1}, which could arise from the vibrational modes of NH_4^+ counterions in close proximity to the negatively charged NCs.[39] Other features in the FTIR spectrum could be assigned to the vibrational motions of residual NMF. Similar to other anionic inorganic ligands, the I^- ions bound to the NC surface could form an electrical double layer around each NC, resulting in a negative ζ-potential (−28.0 mV) sufficient for the electrostatic stabilization of NCs in NMF (Figure S1b). The TEM image (Figure 1e) confirmed that the I^--capped CdSe NCs retained their morphology, except for a shorter interparticle distance. The reduction in interparticle distance was due to the replacement of bulky hydrocarbons by short I^-, in accordance with previous reports on metal-free chalcogenide ligands or SCN^--capped NCs.[14,15]

CdSe NCs can also be stabilized in the presence of other ammonium halides (NH_4Cl and NH_4Br, Figure 1a). Figure S2 shows the absorption spectra for colloidal solutions of the same CdSe NCs capped with different ammonium halides. In all cases, CdSe NCs retained their excitonic features and colloidal stability in NMF by virtue of the negative halide anions bound to the surface. On the other hand, NH_4^+ cations could be solvated and act as counterions.[13] The replacement of NH_4^+ with other cations (*e.g.*, Na^+ or K^+) should not affect the ligand exchange and phase transfer of CdSe NCs. As a consequence, simple halides such as NaCl or KBr can also serve as inorganic ligands and provide electrostatic stabilization of CdSe NCs (Figure 1b). A control experiment was carried out using KNO_3 (with identical ionic strength) as the ligands. No phase transfer or stabilization of NCs in NMF was observed after stirring the two-phase mixture for several days.

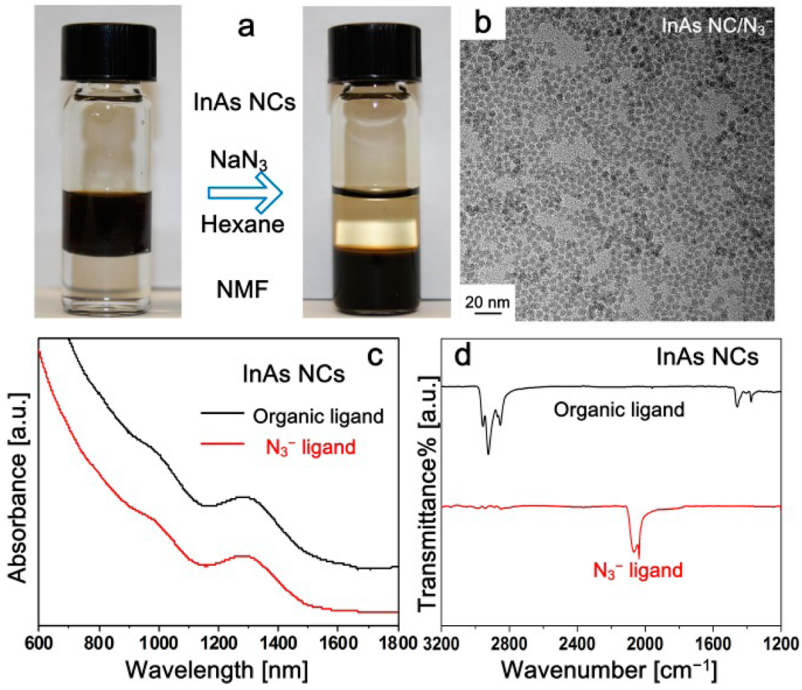

Figure 2. (a) Black-colored solution of InAs NCs transfers from hexane to NMF upon exchange of original organic ligands with NaN_3. (b) TEM image of InAs NCs capped with N_3^- ligands. (c) Absorption spectra of InAs NCs capped with organic ligands and N_3^- in toluene and NMF, respectively. (d) FTIR spectra of InAs NCs capped with organic and N_3^- ligands. The pair of peaks at ~2000−2100 cm^{-1} corresponds to the N_3^- ligands in surface-bound and dissociated (or free ligands) forms, respectively. The FTIR spectra were collected from NC samples embedded in a pressed KBr pellet.

These observations suggest that the stabilization of CdSe NCs is mainly attributed to the binding of negatively charged halide ions (I^-, Br^-, Cl^-) instead of an increase in ionic strength or other factors.

Halide ions can stabilize various NCs in NMF. For instance, Figure S3a and b show the TEM images of CdTe tetrapods capped with organic ligands and NH_4I, respectively. No change in the size or shape was observed after ligand exchange. The absorption spectrum of I^--capped CdTe tetrapods resembled that of organically capped NCs in toluene (Figure S3c). In addition, the XRD pattern suggests no change in crystal size or the formation of impurity phases (Figure S3d). Halide ligands can also work well for spherical CdTe NCs, as was evidenced by the CdTe NCs capped with Cl^- ligands (Figure S4a). Simple halide ligand exchange can be extended to III−V and IV−VI NCs. InAs NCs retained their absorption features and crystal size after the original TOP ligands were replaced with NH_4Cl (Figure S4b). PbTe NCs capped with I^- (Figure S4c) showed unchanged mean size and monodispersity compared to the original NCs. The success of ligand exchange of various types of NCs with simple halide ligands not only facilitates interparticle electronic coupling but also introduces an additional degree of control in surface passivation or remote doping in the NC system. For instance, Cl^- (in the form of $CdCl_2$) is widely used to passivate the CdTe grains for significantly improved efficiency in solar cells.[40] Accordingly, Cl^--capped CdTe NCs could be promising precursors for solution-processed NC solar cells.[41,42]

Pseudohalide Ligands (N_3^-, CN^-). Pseudohalides (CN^-, SCN^-, N_3^-, *etc.*) share similar behavior and chemical properties with halides. In principle, these negatively charged ions may also provide electrostatic stabilization for NCs if a bond forms between the anionic ligands and NCs. Previous reports by the Murray and Kagan group revealed that SCN^- successfully stabilizes NCs and substantially decreases interparticle distance, leading to strong electronic communications between NCs.[15,18,19] In this work, we focus on a specific pseudohalide, azide (N_3^- from sodium azide, NaN_3), due to its clean and complete decomposition upon heating. (*Caution! Sodium azide is toxic and explosive at high temperatures. It must be handled with care.*) It is the first example of "group VA" (pnictides) ligands stabilizing NCs in polar solvents.

Ligand exchange of NCs with NaN_3 was carried out in a similar manner with halide ligand exchange. Upon vigorous stirring, the original organic ligands remained in the upper hexane phase, while the NCs turned hydrophilic and stable in the bottom NMF phase (Figure 2a). Figure 2b shows the TEM image of N_3^--capped InAs NCs, where no obvious changes in size or monodispersity were found when compared to the original NCs (Figure S5a). InAs NCs also retained their electronic structure and size distribution, as evidenced by the excitonic features in the absorption spectra (Figure 2c). Crystal structure and crystalline size were preserved during ligand exchange, according to the XRD data (Figure S5b). FTIR spectra of InAs NCs

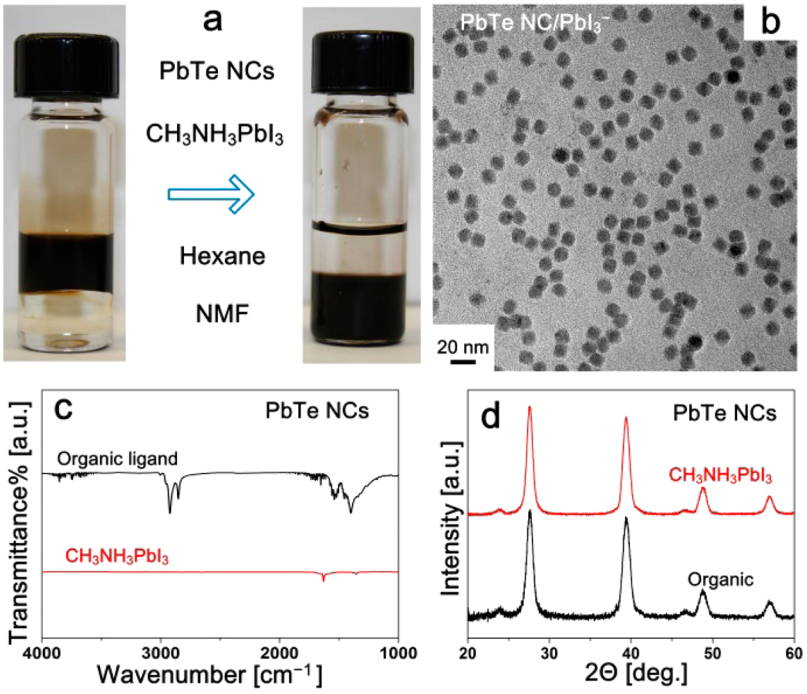

Figure 3. (a) Phase transfer of PbTe NCs from hexane to NMF in the presence of $CH_3NH_4PbI_3$ ligands. (b) TEM image of PbI_3^--capped PbTe NCs. (c) FTIR spectra and (d) XRD reflections of PbTe NCs with original organic and PbI_3^- ligands.

(Figures 2d and S5c) were collected to monitor the replacement of original TOP ligands by N_3^-. The strong bands arising from C–H vibrations between 3000–2800 cm^{-1} and ~1500 cm^{-1} almost disappeared after ligand exchange. More interestingly, a pair of peaks at 2100–2000 cm^{-1} was observed, both of which could be attributed to the stretching modes in N_3^-. On the one hand, the very sharp peak at 2040 cm^{-1} was in accordance with the vibrational peak of pure NaN_3 (Figure S5c), which comes from either free residual NaN_3 after ligand exchange or N_3^- ligands dissociated from the surface of the NCs. On the other hand, the much broader peak at higher frequency (~2070 cm^{-1}) can be assigned to the N_3^- ligands covalently bound to the positively charged sites on the NC surface, where the shift in frequency may come from the binding of N_3^- on the NC surface. A previous report by the Murray and Kagan group explicitly investigated the FTIR spectra of NCs capped with SCN^- ligands, where the broadening of absorption peaks of bound SCN^- ligands and a shift in vibrational frequencies for ligands in different status (bound, dissociated, or free ligands) were also observed.[15] The FTIR spectra (Figures 2d and S5c) suggest that the N_3^- ligands are bound to the InAs NC surface and enable the electrostatic stabilization of NCs in NMF (ζ-potential ≈ −29.3 mV, Figure S5d). A similar ligand exchange procedure was performed on InP and CdSe NCs, the characterizations of which are shown in Figures S6 and S7, respectively.

Besides azides, other pseudohalides such as cyanide (CN^-) can also serve as capping ligands for NCs. For example, a complete phase transfer was observed on CdSe NCs from hexane to NMF in the presence of NaCN. The CN^--capped CdSe NCs showed good colloidal stability, and the absorption spectra indicated that the excitonic features were preserved (Figure S8). (*Caution! Sodium cyanide is highly toxic. It must be handled with care and proper protections.*)

Halometallate Ligands (*e.g.*, PbI_3^-). Recently, strikingly rapid progress in the field of solar cells has been achieved since the use of inorganic–organic hybrid haloplumbates (with perovskite crystal structure) as the light-harvesting materials.[43] Devices with $CH_3NH_3PbI_3$[44,45] or $CH_3NH_3PbI_{3-x}Cl_x$[46] as the active layer were reported to have remarkable energy conversion efficiencies exceeding 15%. Based on the success of surface chemistry with short halide and pseudohalide ligands, it is reasonable to expect that bulky haloplumbates (*e.g.*, PbI_3^-) could perform well as ligands for NCs. During our preparation of this paper, a report by Dirin *et al.* proved the feasibility of using lead halide perovskites and several other metal halide complexes as inorganic capping ligands for NCs while retaining high efficiency in photoluminescence.[35] In our work, haloplumbates ($CH_3NH_3PbI_3$, *etc.*) were synthesized using the method described in previous reports.[47,48] Electrospray ionization mass spectrometry (ESI-MS) analysis of $CH_3NH_3PbI_3$ solution shows that PbI_3^- anions are the main fragments under the measurement conditions (Figure S9). Figure 3a shows the phase transfer of PbTe NCs from hexane to NMF in the presence of $CH_3NH_3PbI_3$. The phase transfer occurred soon after the two phases mixed, leading to a stable colloidal solution of PbTe

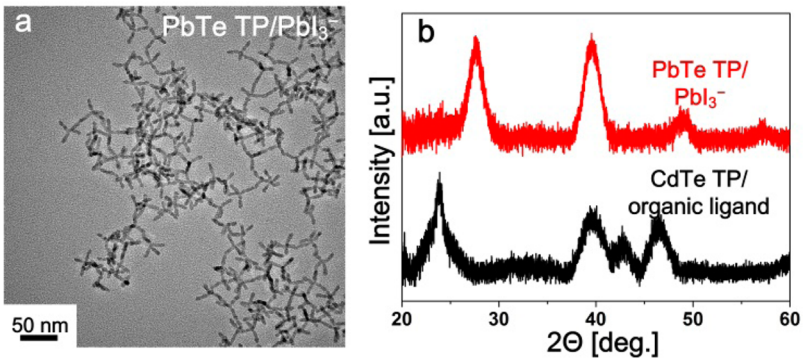

Figure 4. (a) TEM image of PbTe tetrapods after the ligand/cation exchange of CdTe tetrapods with $CH_3NH_4PbI_3$ ligands. (b) XRD patterns of CdTe tetrapods before and after the ligand exchange with $CH_3NH_4PbI_3$, showing a complete conversion from CdTe to PbTe tetrapods.

NCs in NMF. A stable solution of PbTe NCs in NMF was also obtained when other haloplumbates (*e.g.*, $CH_3NH_3PbI_2Cl$, $CH_3NH_3PbBr_3$) were used as the ligand. As observed in the TEM image (Figure 3b), the PbI_3^--capped PbTe NCs maintained their size monodispersity. The ζ-potential for PbI_3^--capped PbTe NCs (*ca.* −50 mV) was substantially higher than that of I^--capped PbTe NCs (*ca.* −15 mV), presumably due to stronger binding (Figure S10). The phase transfer of PbTe NCs from hexane to NMF resulted in a complete disappearance of vibrational bands corresponding to C−H stretching and bending, respectively (Figure 3c). In addition, no reflections other than PbTe were observed in the XRD pattern after PbI_3^- ligand exchange, while crystal size remained unchanged (Figure 3d). Stable solutions were also obtained in several other combinations of PbCh NCs and haloplumbates, as shown in Table S1. On the basis of previous reports, solution phase ligand exchange of PbCh NCs (especially PbSe or PbTe NCs) with inorganic ligands usually fails to yield stable solutions, except *via* select ligands (*e.g.*, for PbTe: Sb_2Te_3-MCC[38] or Te^{2-} [14]). The haloplumbate ligands (or, more extensively, halometallates) significantly enrich the toolbox for solution-processed all-inorganic PbCh NC solids.

A similar ligand exchange process with haloplumbates was also carried out with II−VI NCs. A complete cation exchange took place simultaneously with the phase transfer (also observed in the recent work by Dirin *et al.*[35]), converting cadmium chalcogenide (CdCh) NCs into corresponding PbCh ones while preserving the morphology of the original NCs. For instance, the size and shape of the CdTe tetrapods were unaltered after ligand/cation exchange with $CH_3NH_3PbI_3$ (Figure 4a), whereas a phase transition from wurtzite CdTe to rock salt PbTe was detected (Figure 4b). As a result, PbTe tetrapods capped with PbI_3^- ligands in NMF were obtained. Simultaneous phase transfer and cation exchange from Cd^{2+} to Pb^{2+} was also observed in the case of CdSe NCs (Figure S11). Efficient cation exchange of NCs with a substitutional ion from solution has been well studied, as exemplified by reversible conversion from CdSe NCs to Ag_2Se NCs.[49] However, according to previous reports, cation exchange from Cd^{2+} to Pb^{2+} cannot be accomplished without the Cu^{2+} intermediates.[50] A tentative explanation for the observations in this work is that the combination of haloplumbates and hexane/NMF solvent provides an adequate difference in the solvation energy of Cd^{2+} and Pb^{2+}, driving the complete cation exchange and the formation of PbCh NCs. This demonstrates a facile route to build anisotropic, all-inorganic PbCh nanostructures, which are of great importance in various applications.

Charge Transport in Arrays of I^--Capped CdSe and N_3^--Capped InAs NCs. As discussed above, the halide and pseudohalide ligands can bind to the NC surface and stabilize various NCs by electrostatic repulsion (Table S1). The exchange of bulky and insulating organic surfactants with short halide and pseudohalide (*e.g.*, I^- or N_3^-) ligands should substantially improve electronic communication between individual NCs. Similar behavior has been observed for devices made of NCs capped with short inorganic ligands including MCCs,[17,22] metal-free chalcogenides,[14,17] and SCN^- anions.[18,19] For charge transport studies, we prepared field effect transistor (FET) devices made of closely packed, NH_4I-capped CdSe and NaN_3-capped InAs NCs using highly doped, SiO_2-coated silicon wafers as substrates. The NC solutions in NMF were spin-coated at an elevated temperature (70 °C) to form ∼30−40 nm thick films, which significantly exceeded the depth of the accumulation layer formed upon applied gate bias. The thin films were annealed at 100 °C for 1 h to evaporate residual solvents and then annealed at various temperatures (150, 200, 250, 300, or 350 °C) for 30 min to improve electrical characteristics of NC films (see Experimental Section for more details). Source and drain Al contacts were deposited on top of the NC thin films through a shadow mask using a thermal evaporation system. All FET fabrication and measurement steps were performed in a N_2-filled glovebox. In line with previous studies, the thermal annealing of halide- and pseudohalide-capped NC thin films under inert

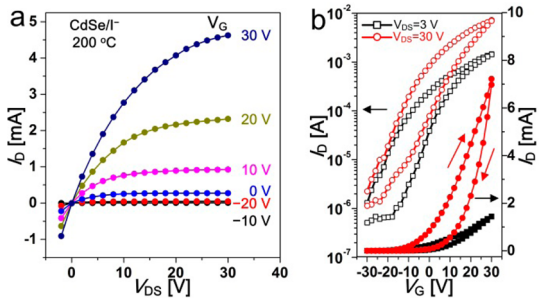

Figure 5. Output (a) and transfer (b) characteristics of I^--capped CdSe NC FETs annealed at 200 °C. (a) Plots of the drain current (I_D) *vs* drain−source voltage (V_{DS}) measured at different gate voltages (V_G). (b) Plots of I_D *vs* V_G for the calculation of current modulation and electron mobility at a constant V_{DS} = 3 V for linear regime and V_{DS} = 30 V for saturation regime. The channel width and length are 1500 and 30 μm, respectively. The thickness of SiO_2 gate dielectrics is 100 nm.

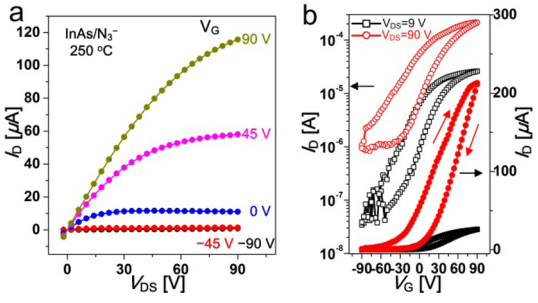

Figure 6. Output (a) and transfer (b) characteristics of N_3^--capped InAsNC FET annealed at 250 °C. (a) Plots of I_D *vs* V_{DS} measured at different V_G. (b) Plots of I_D *vs* V_G for the calculation of current modulation and electron mobility at a constant V_{DS} = 9 V for linear regime and V_{DS} = 90 V for saturation regime. The channel width and length are 1500 and 60 μm, respectively. The thickness of SiO_2 gate dielectrics is 300 nm.

atmosphere led to the evaporation of residual solvent molecules bound on the NC surface, changes in surface chemistry, and sintering of NCs (at very high temperatures).

Figure 5a,b shows the representative output and transfer characteristics for a FET device assembled from NH_4I-capped CdSe NCs and annealed at 200 °C for 30 min. Annealing at 200 °C led to unaltered widths of XRD peaks (Figure S12a). The estimated crystal size by Scherrer's equation was identical to that of the original NCs (~3.4 nm, Figure S12b). The output and transfer characteristics clearly show n-type current modulations with good linear/saturation behavior and on/off current ratios (I_{On}/I_{Off}) of 10^3−10^4. The electron mobility was found to be $\mu_{lin} \approx 12.8$ cm^2 V^{-1} s^{-1} in the linear regime (drain−source voltage, V_{DS} = 3 V) and $\mu_{sat} \approx 5.0$ cm^2 V^{-1} s^{-1} in the saturation regime (V_{DS} = 30 V). These mobility values were comparable with those of the best thin film devices assembled from inorganically capped CdSe NCs (~20 cm^2 V^{-1} s^{-1} for CdSe NCs capped with $In_2Se_4^{2-}$[17] or SCN^-[18,19]) and were several times higher compared to the S^{2-}-capped CdSe NC based devices (~2 cm^2 V^{-1} s^{-1}[13,14]). Considering the simplicity and accessibility of the ammonium halide ligands, this technique could provide a useful solution-based approach in the fabrication of high-performance thin film electronics.

We also investigated the effect of annealing temperature on the FET performance of I^--capped CdSe NCs, as summarized in Table S2. The thin film annealed at 150 °C preserved the grain size of the NCs, as evidenced by the XRD pattern (Figure S12). Remarkably, the electron mobility approached ~1.6 cm^2 V^{-1} s^{-1} in the linear regime and ~1.4 cm^2 V^{-1} s^{-1} in the saturation regime of FET operations, respectively (Figure S13 and Table S2). The improved FET performance of 200 °C annealed devices compared to the ones annealed at 150 °C could be attributed to the more efficient evaporation of residual solvent molecules on the NC surface and the desorption/decomposition of inorganic ligands at elevated temperatures. In addition, cross-linking or necking of I^--capped CdSe NCs might occur after mild annealing (150 or 200 °C), while individual grain size was maintained according to the XRD analysis. In both cases, decreased interparticle distance and the resulting improved electronic coupling can be expected. On the other hand, thin films annealed at 300 °C showed further improved electron mobilities with remarkably reduced hysteresis in transfer characteristics (Figure S13 and Table S2: $\mu_{lin} \approx 30.8$ cm^2 V^{-1} s^{-1} and $\mu_{sat} \approx 10.3$ cm^2 V^{-1} s^{-1}). However, significant narrowing in XRD peaks was observed (Figure S12), which indicates NC sintering and the crystal grain size increased from ~3.4 nm to ~6.5 nm. As a consequence, the enhanced electron transport with reduced hysteresis might be related to the increase in grain size and reduced number of grain boundaries along the electron path.

FET devices made of N_3^--capped InAs NCs (annealed at 250, 300, or 350 °C) also showed n-type transport behavior (Figure 6a,b and Figure S14). After the films were annealed at 250 or 300 °C, the XRD pattern of NaN_3-capped InAs NCs showed no narrowing in reflections, which can be interpreted as the absence of NC sintering (Figure S15). At the same time, the inorganically capped N_3^- ligands could be efficiently decomposed into nitrogen, leading to decreased interparticle distance and improved electron coupling. As a result, the device annealed at 250 °C showed $\mu_{lin} \approx 0.16$ cm^2 V^{-1} s^{-1} together with an $I_{On}/I_{Off} \approx 10^3$ at a fixed V_{DS} = 9 V. When the annealing temperature increased to 350 °C, a slight increase in the carrier mobility was observed, but the NCs also started to sinter at this temperature (grain size from 3.6 to 4.3 nm) (Figures S14 and S15). The combination of N_3^- ligands and InAs NCs suggests an opportunity to obtain prototypical "all III−V" NC solids by removing residual Na^+ counterions. A previous study on Ge_9^{7-} Zintl clusters has shown effective replacement of cationic species using ion-exchange resin.[51] We extend this resin-based cation exchange technique to the solution of NaN_3-capped InAs

TABLE 1. Elemental Analysis of N_3^--Capped InAs NCs

InAs NCs	In/As (molar ratio)	Na/As (molar ratio)
organic-capped	1.3	0
NaN_3-capped	1.3	0.13
NH_4N_3-capped	1.2	0.06

NCs (see Experimental Section). Our preliminary results showed an over 50% replacement of Na^+ by the volatile NH_4^+ cations using resin (Table 1) while the colloidal stability of InAs NCs in NMF was maintained. Our ultimate goal is to completely replace Na^+ by volatile cations (*e.g.*, NH_4^+) or group IIIA cations (*e.g.*, In^{3+}, Ga^{3+}) and construct "all III−V" semiconductor nanostructures.

CONCLUSIONS

In conclusion, we have demonstrated that various halide, pseudohalide, and halometallate ligands can bind to the surface of NCs. They provide colloidal stability for NC dispersions in NMF and preserve the electronic structures of individual NCs. Simple halide ligands (*e.g.*, NH_4I) represent a useful class of short, robust, and nontoxic inorganic ligands for solution phase ligand exchange, while the azide anion (N_3^-) is the first example of "group VA" ligands for NCs. The compact halide and pseudohalide ligands shorten interparticle distance and improve electronic coupling between adjacent NCs, leading to high carrier mobility. For instance, I^--capped CdSe NC arrays showed a high field-effect electron mobility of ~12 $cm^2\ V^{-1}\ s^{-1}$, which is comparable to record mobilities for solution-processed NC arrays. Meanwhile, N_3^--capped InAs NCs suggest the potential fabrication of "all III−V" NC solids (*e.g.*, InAs/InN or InAs/GaN heterostructures by introducing In^{3+} or Ga^{3+} cations). Lastly, we have explored the possibility of stabilizing PbCh NCs with lead halide based halometallate (*e.g.*, $CH_3NH_3PbI_3$) ligands. These halide, pseudohalide, and halometallate ligands can enrich the current ligand chemistry of all-inorganic NCs and suggest promising applications in electronic, optoelectronic, and thermoelectric devices.

EXPERIMENTAL SECTION

Nanocrystal Synthesis. Wurtzite CdSe NCs capped with ODPA were synthesized from CdO and *N*-trioctylphosphine selenide (TOPSe) according to the report from Manna *et al.*[52] Wurtzite CdSe NCs capped with OA were synthesized using cadmium oleate as the precursor of Cd. In brief, 1.2 g of TOPO, 2.25 mL of cadmium oleate solution in OA, and 12 mL of octadecene (ODE) were loaded in a 100 mL three-necked flask and dried under vacuum at 70 °C for 1 h. Afterward, the solution was heated to 300 °C under nitrogen. A stock solution containing 4 mL of 1.0 M TOPSe solution in TOP and 3 mL of OAm was swiftly injected at 300 °C. The mixture was kept at 280 °C for 2−3 min and quickly cooled to room temperature. The CdSe NCs can be isolated by adding ethanol to the crude solution followed by centrifugation and redispersed in common solvents such as hexane. The washing procedure with ethanol and hexane was repeated three more times to remove excess ligands. The purified CdSe NCs were dissolved in hexane. Spherical CdTe NCs and CdTe tetrapods were synthesized using the method described by Yu *et al.*[53] InAs NCs capped with TOP were prepared using a modified recipe of Guzelian *et al.*[54] InP NCs capped with TOP and TOPO were synthesized following a slightly modified method reported by Micic *et al.*[55] Detailed synthetic methods for InAs and InP NCs were provided in our previous report.[22] PbTe NCs were synthesized using a slightly modified recipe by Urban *et al.*,[56] as described in ref 38. PbS NCs were synthesized according to the protocol developed by Hines *et al.*[57]

Ligand Exchange. The ligand exchange process was performed under inert atmosphere in a N_2-filled glovebox. NCs capped with organic ligands were dissolved in hexane, while halide-related ligands (ligand/NC ≈ 0.5−5 in weight, depending on the combination of NCs and ligands, size, shape, and concentration of NCs, *etc.*) were dissolved in NMF. In a typical ligand exchange of OA-capped CdSe NCs with NH_4I, 1 mL of CdSe NC solution in hexane (~10 mg/mL) was mixed with 1 mL of NMF containing excess NH_4I (~20−30 mg). Upon vigorous stirring, the NCs gradually transferred from hexane to NMF, resulting in a colorless top phase within 1 h. The bottom phase was separated and rinsed with fresh hexane three times. Afterward, the I^--capped CdSe NCs were precipitated out by adding toluene (2−3 mL). The NC precipitates can redisperse in NMF (0.1−1 mL) and form a stable solution (up to ~100 mg/mL) for at least several weeks. Ligand exchange of other combinations of NCs (CdTe, InAs, InP, PbTe, PbS) and ligands (NH_4X, NaN_3, NaCN, $CH_3NH_3PbX_3$ (X = Cl, Br, I)) was carried out in a similar way (see Table S1). The phase transfer may take from several minutes to several hours, depending on a number of factors such as the nature of the original organic ligands and incoming inorganic ligands, the amount of residual organic ligands on the NC surface prior to ligand exchange, the size and concentration of NCs, and so forth.

Characterization Techniques. Transmission electron microscopy (TEM) images of NCs were obtained using a 300 kV FEI Tecnai F30 microscope. Wide angle powder X-ray diffraction patterns were collected using a Bruker D8 diffractometer with a Cu Kα X-ray source operating at 40 kV and 40 mA. Thin film samples were prepared by drop casting NC solutions on a silicon substrate and then drying at ~70 °C in a N_2-filled glovebox. Prior to sample preparation, the NCs were thoroughly washed to remove any residual inorganic ligands. In detail, after the phase transfer into NMF and a triple rinse with hexane, the NCs were precipitated out by adding toluene and redispersed in NMF. In some cases, one more cycle of precipitation/redispersion was required for a complete removal of residual inorganic ligands. To investigate the evolution of the size of I^--capped CdSe NCs and N_3^--capped InAs NCs during thermal annealing, the thin films were annealed at various temperatures on top of a hot plate in a glovebox. The size of the NCs was estimated from the widths of the XRD peaks (from 40° to 50°) using Scherrer's equation. Inductively coupled plasma optical emission spectroscopy (ICP-OES) analysis was carried out on an Agilent 700 Series to investigate the Na content in N_3^--capped InAs NCs before and after NH_4^+ cation exchange. Samples were digested by a mixture of deionized ultrafiltered water and aqua regia (HNO_3, ≥69.0%, TraceSELECT, for trace analysis, Sigma-Aldrich; HCl, ≥37%, TraceSELECT, for trace analysis, fuming, Sigma-Aldrich) in a plastic container. Note that glass containers may release Na^+ and interfere with the detection of Na. The optical absorption spectra were collected using a Cary 5000 UV−vis−NIR spectrophotometer. Fourier-transform infrared spectra were acquired in transmission mode using a Nicolet Nexus-670 FTIR spectrometer. Samples for FTIR measurements were mostly prepared by drop casting concentrated NC dispersions on KBr crystal substrates (International Crystal Laboratories) and were then dried at 120 °C under vacuum to remove most of the NMF solvent. IR absorbance was normalized to the weight of

absorbing material deposited per unit area of the substrate. To quantitatively compare IR spectra, we applied standard background subtraction and baseline correction routines. For FTIR analysis on N_3^--capped InAs or InP NCs, NCs were precipitated out from the NMF solution and thoroughly dried. The NC solids was then mixed with KBr powder and pressed into a pellet. In the control experiment, a NaN_3 pellet was prepared from a mixture of NaN_3 and KBr powder. Zeta-potential (ζ-potential) data were collected using a Zetasizer Nano-ZS (Malvern Instruments, UK). Electrospray ionization mass spectrometry of $CH_3NH_3PbI_3$ was performed using an Agilent 1100 LC/MSD mass spectrometer. $CH_3NH_3PbI_3$ was dissolved in γ-butyrolactone or NMF (~1 mg/mL), and pure acetonitrile was selected as the carrier fluid. The data were acquired in the negative ion mode with a fragmentor of 0 V. The peak assignments were based on the comparison of experimental mass spectra with calculated isotope patterns.

Field Effect Transistor Device Fabrication and Electrical Measurements. Prime grade, n-type arsenic doped Si wafers with 100 nm thick SiO_2 gate dielectrics (<0.005 Ω cm, NamKang High-Tech) and with 300 nm thick SiO_2 (0.001–0.005 Ω cm, Silicon Inc.) were used as gate substrates. The substrates were cleaned by piranha treatment followed by multiple rinses with DI water before use. Solutions of I^--capped CdSe NCs (~70 mg/mL in NMF) and N_3^--capped InAs NCs (~50 mg/mL in NMF) were spin-coated (spread: 600 rpm, 6 s; spin: 2000 rpm, 60 s) on the cleaned substrates, which produced ~30–40 nm thick NC films. A 500 W infrared lamp was used to maintain the temperature of solutions and substrates at ~70 °C during spin-coating due to the high boiling point of NMF (~183 °C). The NC films were annealed at 100 °C for 1 h to evaporate residual solvents and then annealed at 150, 200, 250, 300, or 350 °C for 30 min to improve electrical characteristics of NC films. Al source/drain electrodes of 100 nm thick were deposited through a shadow mask using a thermal evaporator to complete a top-contact, bottom-gate FET structure (channel width W = 1500 μm and channel length L = 30, 60, or 125 μm). All fabrication steps except substrate cleaning were performed in a N_2-filled glovebox.

FET measurements were performed using a semiconductor analyzer (Agilent B1500A) in a N_2-filled glovebox. The linear and saturation regime FET mobility was calculated by fitting the experimental data to the following equations: $\mu = (L/WC_iV_{DS})(dI_{DS}/dV_G)$ for the linear regime and $I_D = \mu C_i(W/2L)(V_G - V_{Th})^2$ for the saturation regime, where V_{Th}, C_i, V_{DS}, I_D, and V_G are the threshold voltage, capacitance per unit area, drain–source voltage, drain current, and gate voltage, respectively.

Brief Description of the Cation Exchange of InAs/N_3^-/Na^+ NCs with NH_4^+. NH_4^+-resin was prepared by mixing the acidic resin beads (Amberlyst 15 hydrogen form, Fluka) with an aqueous solution of NH_4Cl (~0.2–0.3 M, pH ~4–5). The mixture was sonicated for several minutes, and the resin beads were separated from the solution by centrifugation. The pH of the supernatant was <1, indicating the elution of H^+ from the acidic resin and the successful substitution of H^+ by NH_4^+. This procedure was repeated five times. Finally, the NH_4^+-resin was washed by DI water to remove any residual, free NH_4Cl and dried under vacuum.

The cation exchange of N_3^--capped InAs NCs was carried out in the glovebox. In detail, ~30 mg of NH_4^+-resin beads was added to a 1.0 mL NMF solution of N_3^--capped InAs NCs (~5 mg/mL, with Na^+ as the counterions). The mixture was vigorously vortexed for ~10–15 min, and the stable NC solution was separated from the resin beads by centrifugation. The InAs/N_3^-/NH_4^+ NCs were retrieved by adding toluene to the solution followed by centrifugation and formed a stable solution in ~0.1 mL of NMF. An ICP-OES analysis (Table 1) on the InAs/N_3^-/Na^+ and InAs/N_3^-/NH_4^+ NCs suggests ~30–40 N_3^- ligands per InAs NC and a more than 50 mol % reduction in Na content after the NH_4^+ cation exchange.

Conflict of Interest: The authors declare no competing financial interest.

Supporting Information Available: Additional experimental details, figures, and tables as described in the text. This material is available free of charge *via* the Internet at http://pubs.acs.org.

Acknowledgment. We thank C. Jiang, J. Son, M. Panthani, and M. Boles for helpful discussions and T. Shpigel for editing the manuscript. The work on II–VI and IV–VI nanomaterials was supported by the DOE SunShot program under Award No. DE-EE0005312 and by the II–VI Foundation. The work on III–V nanomaterials was supported by NSF under Award No. DMR-1310398 and DOD ONR Award No. N00014-13-1-0490. D.V.T. also thanks the David and Lucile Packard Foundation and Keck Foundation for their generous support. This work used facilities supported by the NSF MRSEC Program under Award No. DMR 08-20054. The work at the Center for Nanoscale Materials (ANL) was supported by the U.S. Department of Energy under Contract No. DE-AC02-06CH11357.

REFERENCES AND NOTES

1. Talapin, D. V.; Murray, C. B. PbSe Nanocrystals Solids for *n*- and *p*-Channel Thin Film Field-Effect Transistors. *Science* **2005**, *310*, 86–89.
2. Yu, D.; Wang, C.; Guyot-Sionnest, P. *n*-Type Conducting CdSe Nanocrystal Solids. *Science* **2003**, *300*, 1277–1280.
3. Law, M.; Luther, J. M.; Song, Q.; Hughes, B. K.; Perkins, C. L.; Nozik, A. J. Structural, Optical, and Electrical Properties of PbSe Nanocrystal Solids Treated Thermally or with Simple Amines. *J. Am. Soc. Chem.* **2008**, *130*, 5974–5985.
4. Coe, S.; Woo, W.-K.; Bawendi, M.; Bulovic, V. Electroluminescence from Single Monolayers of Nanocrystals in Molecular Organic Devices. *Nature* **2002**, *420*, 800–803.
5. Gur, I.; Fromer, N. A.; Geier, M. L.; Alivisatos, A. P. Air-Stable All-Inorganic Nanocrystal Solar Cells Processed from Solution. *Science* **2005**, *310*, 462–465.
6. Konstantatos, G.; Howard, I.; Fischer, A.; Hoogland, S.; Clifford, J.; Klem, E.; Levina, L.; Sargent, E. H. Ultrasensitive Solution-Cast Quantum Dot Photodetectors. *Nature* **2006**, *442*, 180–183.
7. McDonald, S. A.; Konstantatos, G.; Zhang, S.; Cyr, P. W.; Klem, E. J. D.; Levina, L.; Sargent, E. H. Solution-Processed PbS Quantum Dot Infrared Photodetectors and Photovoltaics. *Nat. Mater.* **2005**, *4*, 138–142.
8. Wang, R. Y.; Feser, J. P.; Lee, J.-S.; Talapin, D. V.; Segalman, R.; Majumdar, A. Enhanced Thermopower in PbSe Nanocrystal Quantum Dot Superlattices. *Nano Lett.* **2008**, *8*, 2283–2288.
9. Ko, D.-K.; Kang, Y.; Murray, C. B. Enhanced Thermopower *via* Carrier Energy Filtering in Solution Processable Pt-Sb_2Te_3 Nanocomposites. *Nano Lett.* **2011**, *11*, 2841–2844.
10. Talapin, D. V.; Lee, J.-S.; Kovalenko, M. V.; Shevchenko, E. V. Prospects of Colloidal Nanocrystals for Electronic and Optoelectronic Applications. *Chem. Rev.* **2010**, *110*, 389–458.
11. Kovalenko, M. V.; Scheele, M.; Talapin, D. V. Colloidal Nanocrystals with Molecular Metal Chalcogenide Surface Ligands. *Science* **2009**, *324*, 1417–1420.
12. Kovalenko, M. V.; Bodnarchuk, M. I.; Zaumseil, J.; Lee, J.-S.; Talapin, D. V. Expanding the Chemical Versatility of Colloidal Nanocrystals Capped with Molecular Metal Chalcogenide Ligands. *J. Am. Soc. Chem.* **2010**, *132*, 10085–10092.
13. Nag, A.; Chung, D. S.; Dolzhnikov, D. S.; Dimitrijevic, N. M.; Chattopadhyay, S.; Shibata, T.; Talapin, D. V. Effect of Metal Ions on Photoluminescence, Charge Transport, Magnetic and Catalytic Properties of All-Inorganic Colloidal Nanocrystals and Nanocrystal Solids. *J. Am. Soc. Chem.* **2012**, *134*, 13604–13615.
14. Nag, A.; Kovalenko, M. V.; Lee, J.-S.; Liu, W.; Spokoyny, B.; Talapin, D. V. Metal-Free Inorganic Ligands for Colloidal Nanocrystals: S^{2-}, HS^-, Se^{2-}, HSe^-, Te^{2-}, HTe^-, TeS_3^{2-}, OH^-, and NH_2^- as Surface Ligands. *J. Am. Soc. Chem.* **2011**, *133*, 10612–10620.
15. Fafarman, A. T.; Koh, W.-K.; Diroll, B. T.; Kim, D. K.; Ko, D.-K.; Oh, S. J.; Ye, X.; Doan-Nguyen, V.; Crump, M. R.; Reifsnyder, D. C.; *et al.* Thiocyanate-Capped Nanocrystal Colloids: Vibrational Reporter of Surface Chemistry and Solution-Based Route to Enhanced Coupling in Nanocrystal Solids. *J. Am. Soc. Chem.* **2012**, *133*, 15753–15761.
16. Lee, J.-S.; Kovalenko, M. V.; Huang, J.; Chung, D. S.; Talapin, D. V. Band-Like Transport, High Electron Mobility and High

Photoconductivity in All-Inorganic Nanocrystal Arrays. *Nat. Nanotechnol.* **2011**, *6*, 348–352.
17. Chung, D. S.; Lee, J.-S.; Huang, J.; Nag, A.; Ithurria, S.; Talapin, D. V. Low Voltage, Hysteresis Free, and High Mobility Transistors from All-Inorganic Colloidal Nanocrystals. *Nano Lett.* **2012**, *12*, 1813–1820.
18. Choi, J.-H.; Fafarman, A. T.; Oh, S. J.; Ko, D.-K.; Kim, D. K.; Diroll, B. T.; Muramoto, S.; Gillen, J. G.; Murray, C. B.; Kagan, C. R. Bandlike Transport in Strongly Coupled and Doped Quantum Dot Solids: A Route to High-Performance Thin-Film Electronics. *Nano Lett.* **2012**, *12*, 2631–2638.
19. Kim, D. K.; Lai, Y.; Diroll, B. T.; Murray, C. B.; Kagan, C. R. Flexible and Low-Voltage Integrated Circuits Constructed from High-Performance Nanocrysal Transistors. *Nat. Commun.* **2012**, *3*, 1216.
20. Oh, S. J.; Berry, N. E.; Choi, J.-H.; Gaulding, E. A.; Lin, H.; Paik, T.; Hong, S.-H.; Murray, C. B.; Kagan, C. R. Stoichiometric Control of Lead Chalcogenide Nanocrystal Solids to Enhance Their Electronic and Optoelectronic Device Performance. *ACS Nano* **2013**, *7*, 2413–2421.
21. Oh, S. J.; Berry, N. E.; Choi, J.-H.; Gaulding, E. A.; Lin, H.; Paik, T.; Diroll, B. T.; Muramoto, S.; Murray, C. B.; Kagan, C. R. Designing High-Performance PbS and PbSe Nanocrystal Electronic Devices through Stepwise, Post-Synthesis, Colloidal Atomic Layer Deposition. *Nano Lett.* **2014**, *14*, 1559–1566.
22. Liu, W.; Lee, J.-S.; Talapin, D. V. III–V Nanocrystals Capped with Molecular Metal Chalcogenide Ligands: High Electron Mobility and Ambipolar Photoresponse. *J. Am. Soc. Chem.* **2013**, *135*, 1349–1357.
23. Jang, J.; Liu, W.; Son, J. S.; Talapin, D. V. Temperature-Dependent Hall and Field-Effect Mobility in Strongly Coupled All-Inorganic Nanocrystal Arrays. *Nano Lett.* **2014**, *14*, 653–662.
24. Linder, E.; Picton, H. CLXXXIII—Solution and Pseudo-Solution. Part IV. *J. Chem. Soc.* **1905**, *87*, 1906–1936.
25. Verwey, E. J. W. The Electrical Double Layer and the Stablitiy of Lyophobic Colloids. *Chem. Rev.* **1935**, *16*, 363–415.
26. Peng, H.-C.; Xie, S.; Park, J.; Xia, X.; Xia, Y. Quantitative Analysis of the Coverage Density of Br^- Ions on Pd{100} Facets and Its Role in Controlling the Shape of Pd Nanocrystals. *J. Am. Soc. Chem.* **2013**, *135*, 3780–3783.
27. Tang, J.; Kemp, K. W.; Hoogland, S.; Jeong, K. S.; Liu, H.; Levina, L.; Furukawa, M.; Wang, X.; Debnath, R.; Cha, D.; *et al.* Colloidal-Quantum-Dot Photovoltaics Using Atomic-Ligand Passivation. *Nat. Mater.* **2011**, *10*, 765–771.
28. Owen, J. S.; Park, J.; Trudeau, P.-E.; Alivisatos, A. P. Reaction Chemistry and Ligand Exchagne at Cadmium–Selenide Nanocrystal Surfaces. *J. Am. Soc. Chem.* **2008**, *130*, 12279–12281.
29. Anderson, N. C.; Hendricks, M. P.; Choi, J. J.; Owen, J. S. Ligand Exchange and the Stoichiometry of Metal Chalcogenide Nanocrystals: Spectroscopic Observation of Facil Metal-Carboxylate Displacement and Binding. *J. Am. Soc. Chem.* **2013**, *135*, 18536–18548.
30. Anderson, N. C.; Owen, J. S. Soluble, Chlorine-Terminated CdSe Nanocrystals: Ligand Exchange Monitored by ^1H and ^{31}P NMR Spectroscopy. *Chem. Mater.* **2013**, *25*, 69–76.
31. Ning, Z.; Ren, Y.; Hoogland, S.; Voznyy, O.; Levina, L.; Stadler, P.; Lan, X.; Zhitomirsky, D.; Sargent, E. H. All-Inorganic Colloidal Quantum Dot Photovoltaics Employing Solution-Phase Halide Passivation. *Adv. Mater.* **2012**, *24*, 6295–6299.
32. Ip, A. H.; Thon, S. M.; Hoogland, S.; Voznyy, O.; Zhitomirsky, D.; Debnath, R.; Levina, L.; Rollny, L. R.; Carey, G. H.; Fischer, A.; *et al.* Hybrid Passivated Colloidal Quantum Dot Solids. *Nat. Nanotechnol.* **2012**, *7*, 577–582.
33. Katsiev, K.; Ip, A. H.; Fischer, A.; Tanabe, I.; Zhang, X.; Kirmani, A. R.; Voznyy, O.; Rollny, L. R.; Chou, K. W.; Thon, S. M.; *et al.* The Complete In-Gap Electronic Structure of Colloidal Quantum Dot Solids and Its Correlation with Electronic Transport and Photovoltaic Performance. *Adv. Mater.* **2013**, *26*, 937–942.
34. Bae, W. K.; Joo, J.; Padilha, L. A.; Won, J.; Lee, D. C.; Lin, Q.; Koh, W.-K.; Luo, H.; Klimov, V. I.; Pietryga, J. M. Highly Effective Surface Passivation of PbSe Quantum Dots through Reaction with Molecular Chlorine. *J. Am. Soc. Chem.* **2012**, *134*, 20160–20168.
35. Dirin, D. N.; Dreyfuss, S.; Bodnarchuk, M. I.; Nedelcu, G.; Papagiorgis, P.; Itskos, G.; Kovalenko, M. V. Lead Halide Perovskites and Other Metal Halide Complexes as Inorganic Capping Ligands for Colloidal Nanocrystals. *J. Am. Soc. Chem.* **2014**, *136*, 6550–6553.
36. Zhitomirsky, D.; Furukawa, M.; Tang, J.; Stadler, P.; Hoogland, S.; Voznyy, O.; Liu, H.; Sargent, E. H. N-Type Colloidal-Quantum-Dot Solids for Photovotaics. *Adv. Mater.* **2012**, *24*, 6181–6185.
37. Niu, G.; Wang, L.; Gao, R.; Li, W.; Guo, X.; Dong, H.; Qiu, Y. Inorganic Halogen Ligands in Quantum Dots: I^-, Br^-, Cl^- and Film Fabrication Through Electrophoretic Deposition. *Phys. Chem. Chem. Phys.* **2013**, *15*, 19595–19600.
38. Kovalenko, M. V.; Spokoyny, B.; Lee, J.-S.; Scheele, M.; Weber, A.; Perera, S.; Landry, D.; Talapin, D. V. Semiconductor Nanocrystals Functionalized with Antimony Telluride Zintl Ions for Nanostructured Thermoelectrics. *J. Am. Soc. Chem.* **2010**, *132*, 6686–6695.
39. Bovey, L. F. H. The Infrared Absorption and Reflection Spectra of the Ammonium Halides. *J. Opt. Soc. Am.* **1951**, *41*, 836–848.
40. Al-Allak, H. M.; Brinkman, A. W.; Richter, H.; Bonnet, D. Depedence of CdS/CdTe Thin Film Solar Cell Characteristics on the Processing Conditions. *J. Cryst. Growth* **1996**, *159*, 910–915.
41. Jasieniak, J.; MacDonald, B. I.; Watkins, S. E.; Mulvaney, P. Solution-Processed Sintered Nanocrystal Solar Cells *via* Layer by Layer Assembly. *Nano Lett.* **2011**, *11*, 2856–2864.
42. Panthani, M. G.; Kurley, J. M.; Crisp, R. W.; Dietz, T. C.; Ezzyat, T.; Luther, J. M.; Talapin, D. V. High Efficiency Solution Processed Sintered CdTe Nanocrystal Solar Cells: The Role of Interfaces. *Nano Lett.* **2014**, *14*, 670–675.
43. Kojima, A.; Teshima, K.; Shirai, Y.; Miyasaka, T. Organometal Halide Perovskite as Visible-Light Sensitizers for Photovotaic Cells. *J. Am. Soc. Chem.* **2009**, *131*, 6050–6051.
44. Burschka, J.; Pellet, N.; Moon, S.-J.; Humphry-Baker, R.; Gao, P.; Nazeeruddin, M. K.; Gratzel, M. Sequential Deposition as A Route to High-Performance Perovskite-Sensitized Solar Cells. *Nature* **2013**, *499*, 316–319.
45. Liu, D.; Kelly, T. L. Perovskite Solar Cells with a Planar Heterojunction Structure Prepared Using Room-Temperature Solution Processing Techniques. *Nat. Photonics* **2014**, *8*, 133–138.
46. Liu, M.; Johnston, M. B.; Snaith, H. J. Efficient Planar Heterojunction Perovskite Solar Cells by Vapour Deposition. *Nature* **2013**, *501*, 395–398.
47. Noh, J. H.; Im, S. H.; Heo, J. H.; Mandal, T. N.; Seok, S. I. Chemical Management for Colorful, Efficient, and Stable Inorganic-Organic Hybrid Nanostructured Solar Cells. *Nano Lett.* **2013**, *13*, 1764–1769.
48. Lee, M. M.; Teuscher, J.; Miyasaka, T.; Murakami, T. N.; Snaith, H. J. Efficient Hybrid Solar Cells Based on Meso-Superstructured Organometal Halide Perovskites. *Science* **2012**, *338*, 643–647.
49. Son, D. H.; Hughes, S. M.; Yin, Y.; Alivisatos, A. P. Cation Exchange Reactions in Ionic Nanocrystals. *Science* **2004**, *306*, 1009–1012.
50. Luther, J. M.; Zheng, H.; Sadtler, B.; Alivisatos, A. P. Synthesis of PbS Nanorods and Other Ionic Nanocrystals of Complex Morphology by Sequential Cation Exchange Reactions. *J. Am. Soc. Chem.* **2009**, *131*, 16851–16857.
51. Sun, D.; Riley, A. E.; Cadby, A. J.; Richman, E. K.; Korlann, S. D.; Tolbert, S. H. Hexagonal Nanoporous Germanium through Surfactant-Driven Self-Assembly of Zintl Clusters. *Nature* **2006**, *441*, 1126–1130.
52. Carbone, L.; Nobile, C.; De Giorgi, M.; Sala, D. F.; Morello, G.; Pompa, P.; Hytch, M.; Snoeck, E.; Fiore, A.; Franchini, I. R.; *et al.* Synthesis and Micrometer-Scale Assembly of Colloidal CdSe/CdS Nanorods Prepared by a Seeded Growth Approach. *Nano Lett.* **2007**, *7*, 2942–2950.
53. Yu, W. W.; Wang, Y. A.; Peng, X. Formation and Stability of Size-, Shape, and Structure-Controlled CdTe Nanocrystals:

Ligand Effects on Monomers and Nanocrystals. *Chem. Mater.* **2003**, *15*, 4300–4308.
54. Guzelian, A. A.; Banin, U.; Kadavanich, A. V.; Peng, X.; Alivisatos, A. P. *Appl. Phys. Lett.* **1996**, *69*, 1432–1434.
55. Micic, O. I.; Curtis, C. J.; Jones, K. M.; Sprague, J. R.; Nozik, A. J. Synthesis and Characterization of InP Quantum Dots. *J. Phys. Chem.* **1994**, *98*, 4966–4969.
56. Urban, J. J.; Talapin, D. V.; Shevchenko, E. V.; Murray, C. B. *J. Am. Soc. Chem.* **2006**, *128*, 3248–3255.
57. Hines, M. A.; Scholes, G. D. Colloidal PbS Nanocrystals with Size-Tunable Near-Infrared Emission: Observation of Post-Synthesis Self-Narrowing of the Particle Size Distribution. *Adv. Mater.* **2003**, *15*, 1844–1849.